J|A|C|S
ARTICLES
Published on Web 12/20/2006

Mechanism of Catalytic Aziridination with Manganese Corrole: The Often Postulated High-Valent Mn(V) Imido Is Not the Group Transfer Reagent

Michael J. Zdilla and Mahdi M. Abu-Omar*

Contribution from the Brown Laboratory, Department of Chemistry, Purdue University, 560 Oval Drive,West Lafayette, Indiana 47907

Received September 11, 2006; E-mail: mabuomar@purdue.edu

Abstract: The reaction of ArI═NTs (Ar = 2-(*tert*-butylsulfonyl)benzene and Ts = *p*-toluenesulfonyl) and (tpfc)Mn (tpfc = 5,10,15-tris(pentafluorophenyl)corrole), **1**, affords the high-valent (tpfc)Mn^{V}═NTs, **2**, on stopped-flow time scale. The reaction proceeds via the adduct [(tpfc)Mn^{III}(ArINTs)], **3**, with formation constant $K_3 = (10 \pm 2) \times 10^3$ L mol^{-1}. Subsequently, **3** undergoes unimolecular group transfer to give complex **2** with the rate constant $k_4 = 0.26 \pm 0.07$ s^{-1} at 24.0 °C. The complex (tpfc)Mn catalyzes [NTs] group transfer from ArINTs to styrene substrates with low catalyst loading and without requirement of excess olefin. The catalytic aziridination reaction is most efficient in benzene because solvents such as toluene undergo a competing hydrogen atom transfer (HAT) reaction resulting in H_2NTs and lowered aziridine yields. The high-valent manganese imido complex (tpfc)Mn═NTs does not transfer its [NTs] group to styrene. Double-labeling experiments with ArINTs and $ArINTs^{tBu}$ (Ts^{tBu} = (*p-tert*-butylphenyl)sulfonyl) establish the source of [NR] transfer as a "third oxidant", which is an adduct of Mn(V) imido, [(tpfc)Mn(NTs^{tBu})(ArINTs)] (**4**). Formation of this oxidant is rate limiting in catalysis.

Introduction

Imido complexes of high-valent manganese and iron have been postulated as the active reagents responsible for group transfer in aziridination reactions.[1] For example, Groves and Carreira and co-workers have elegantly implicated Mn^{V}═N(C(O)CF_3) in porphyrin and Schiff base ligand environments, respectively, as group transfer reagent to carbon−carbon double bonds.[2] Even though Mn(V) nitrides have been stabilized by various ancillary ligands, terminal Mn(V) imides are rare.[3] We have been able to obtain isolable Mn(V) imides stabilized by 5,10,15-tris(pentafluorophenyl)corrole (tpfc) via the action of organic aryl azides on Mn(III).[4] More recently Goldberg and co-workers carried out successfully the same reaction with a corrolazine auxiliary ligand.[5] Additionally and only until a few years ago, examples of stable metal imides were extremely rare for the mid-to-late metals of the first-row (3d series).[6,7] Besides their prevalence in catalysis, multiply bonded species, especially for porphyrinoid ligands, play a part in biomimetic and bio-inspired chemistry of metalloenzymes.[8]

For the reasons cited above, the study and characterization of reactive intermediates constitute a major research goal in mechanistic chemistry. The consensus mechanism for atom and group transfer has pointed to L_nM(V)═E (where M = Mn or Fe and E = O or NR) as the oxidizing species.[9,1a,2] Investigation into ruthenium bis(tosylimido porphyrin) complexes have supported this notion.[10] Besides this traditional mechanism, evidence has been reported recently for involvement of a porphyrin metal−oxidant intermediate (eq 1) as a competing oxidant with

(1) (a) Müller, P.; Fruit, C. *Chem. Rev.* **2003**, *103*, 2905. (b) Eikey, R. A.; Abu-Omar, M. M. *Coord. Chem. Rev.* **2003**, *243*, 83.
(2) (a) Groves, J. T.; Takahashi, T. *J. Am. Chem. Soc.* **1983**, *105*, 2073. (b) Du Bois, J.; Tomooka, C. S.; Hong, J.; Carreira, E. M. *Acc. Chem. Res.* **1997**, *30*, 364.
(3) Mn(V) nitrides are know for porphyrin and other ancillary ligands. See for example: (a) Buchler, J. W.; Dreher, C.; Lay, K. L.; Lee, Y. J. A.; Scheidt, W. R. *Inorg. Chem.* **1983**, *22*, 888. (b) Hill, C. L.; Hollander, F. J. *J. Am. Chem. Soc.* **1982**, *104*, 7318. (c) Meyer, K.; Bendix, J.; Metzler-Nolte, N.; Weyhermüller, T.; Wieghardt, K. *J. Am. Chem. Soc.* **1998**, *120*, 7260. (d) Golubkov, G.; Bendix, J.; Gray, H. B.; Mahammed, A.; Goldberg, I.; DiBillio, A. J.; Gross, Z. *Angew. Chem. Int. Ed.* **2001**, *40*, 2132. (e) Chang, C. J.; Connick, W. B.; Low, D. W.; Day, M. W.; Gray, H. B. *Inorg. Chem.* **1998**, *37*, 3107.
(4) Eikey, R. A.; Khan, S. I.; Abu-Omar, M. M. *Angew. Chem. Int. Ed.* **2002**, *41*, 3592.
(5) Lansky, D. E.; Kosack, J. R.; Narducci-Sarjeant, A. A.; Goldberg, D. P. *Inorg. Chem.* **2006**, *45*, 8477.
(6) (a) Glueck, D. S.; Wu, J. X.; Hollander, F. J.; Bergman, R. G. *J. Am. Chem. Soc.* **1991**, *113*, 2041. (b) Verma, A. K.; Nazif, T. N.; Achim, C.; Lee, S. C. *J. Am. Chem. Soc.* **2000**, *122*, 11013.
(7) Recent examples of well-defined multiply bonded terminal ligands have been reported in low coordinate geometries for Fe: (a) Brown, S. D.; Peters, J. C. *J. Am. Chem. Soc.* **2005**, *127*, 1913. (b) Kaizer, J.; Klinker, E. J.; Oh, N. Y.; Rohde, J. U.; Song, W. J.; Stubna, A.; Kim, J.; Münck, E.; Nam, W.; Que, L., Jr. *J. Am. Chem. Soc.* **2004**, *126*, 472. (c) Bart, S. C.; Lobkovsky, E.; Bill, E.; Chirik, P. J. *J. Am. Chem. Soc.* **2006**, *128*, 5302. For Co: (d) Shay, D. T.; Yap, G. P. A.; Zakharov, L. N.; Rheingold, A. L.; Theopold, K. H. *Angew. Chem. Int. Ed.* **2005**, *44*, 1508. (e) Dai, X. L.; Kapoor, P.; Warren, T. H. *J. Am. Chem. Soc.* **2004**, *126*, 4798. (f) Jenkins, D. M.; Betley, T. A.; Peters, J. C. *J. Am. Chem. Soc.* **2002**, *124*, 11238. For Ni: (g) Mindiola, D. J.; Hillhouse, G. L. *J. Am. Chem. Soc.* **2002**, *124*, 9976. (h) Kogut, E.; Wiencko, H. L.; Zhang, L. B.; Cordeau, D. E.; Warren, T. H. *J. Am. Chem. Soc.* **2005**, *127*, 11248.
(8) (a) Groves, J. T. In *Cytochrome P450: Structure, Mechanism, and Biochemistry*, 3rd ed.; Ortiz de Montellano, P. R.; Ed.; Kluwer Academic/Plenum Publishers: New York, 2004; pp 1−44. (b) Collman, J. P.; Boulatov, R.; Sunderland, C. J.; Fu, L. *Chem. Rev.* **2004**, *104*, 561. (c) Denisov, I. G.; Makris, T. M.; Sligar, S. G.; Schlichting, I. *Chem. Rev.* **2005**, *105*, 2253. (d) Costas, M.; Mehn, M. P.; Jensen, M. P.; Que, L., Jr. *Chem. Rev.* **2004**, *104*, 939. (e) Kryatov, S. V.; Rybak-Akimova, E. V.; Schindler, S. *Chem. Rev.* **2005**, *105*, 2175. (f) Abu-Omar, M. M.; Loaiza, A.; Hontzeas, N. *Chem. Rev.* **2005**, *105*, 2227.

the multiply bonded oxo complex.[11] Through convincing isotope labeling experiments, Goldberg and co-workers presented yet another possible "third oxidant" in which the Mn(V) oxo corrolazine forms an adduct with the oxidant, and the oxygen atom of the adduct is the one that transfers to substrate (eq 2).[12]

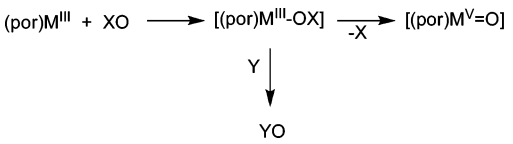

(1)

where por = porphyrin; M = Fe or Mn; XO = H_2O_2, ROOH, or PhI=O; and Y = substrate such as organic sulfides or alkenes.

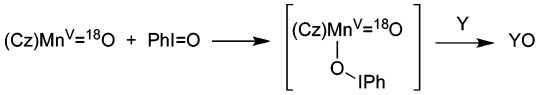

(2)

where Cz = corrolazine and Y = PhSMe.

Our stable and isolable Mn(V) imido corrole complexes are not oxidizing and do not effect [NR] group transfer to organic substrates.[4,13] The synthetic methodology we employed in preparing (tpfc)Mn^V=NR was limited to aryl groups with alkyl or halide substituents in the 2,6-(ortho) positions.[14] Therefore, we reasoned that more electron-withdrawing substituents are needed on the imido ligand such as acyl or tosyl to induce efficient group transfer. These complexes were not possible to synthesize using organic azides because tosyl azide, for example, cannot be easily activated by thermolysis or photolysis.[14] In this work, we report on the reaction of soluble iodonium ylides[15] (ArI=NTs, Ar = 2-(*tert*-butylsulfonyl)benzene and Ts = *p*-toluenesulfonyl) and (tpfc)Mn^{III}, **1**, to afford characterizable Mn^V=NTs, **2** (it should be noted that while we refer formally to Mn^{III} and Mn^V in complexes **1** and **2**, it is possible that a more electronically accurate description for either is the one-electron reduced metal with a corrole radical cation[16]). The manganese corrole complex (tpfc)Mn^{III} is an effective catalyst for group transfer to styrene substrates in benzene. The reaction's main highlights are low catalyst loading and no requirement for excess olefin. When the reaction is conducted in toluene, aziridine yields are lowered because of intervening hydrogen atom transfer (HAT) from the solvent. While the terminal Mn-(V) tosyl imide is reactive toward HAT reactions, it does NOT transfer the terminal tosyl imide ligand to styrene substrates. Furthermore, we present unambiguous evidence through labeling experiments that the oxidant in this system is an iodoimine (ArI=NTs) adduct of (tpfc)Mn^V=NTs, analogous to the "third oxidant" proposed by Goldberg and co-workers.[12]

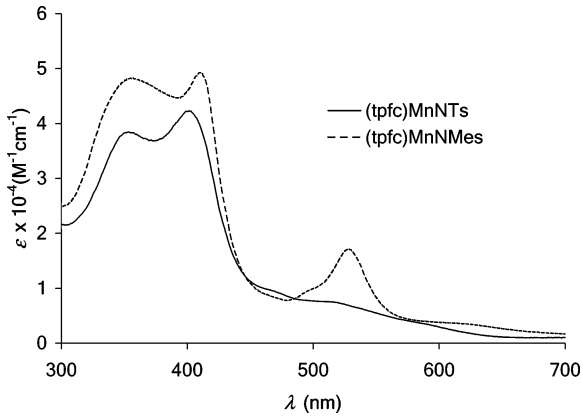

Figure 1. Comparative UV−vis spectra of **2** and (tpfc)MnNMes in acetonitrile.

Results and Discussion

Reaction of (tpfc)Mn^{III}(EtOAc) with ArI=NTs. The manganese(III) complex of tpfc is often written in the literature as [(tpfc)Mn] without specifying axial ligation because crystallization proved difficult without addition of a ligand additive such as $OPPh_3$.[17] We have developed a successful purification/crystallization protocol that affords 5-coordinate manganese with a single axial ethyl acetate ligand (see Supporting Information for structural data). Addition of ArI=NTs or PhI=NTs to (tpfc)-Mn(EtOAc), **1**, at room temperature in a variety of dry organic solvents (CH_2Cl_2, CH_3CN, benzene, or toluene) results in a color change from green to red-brown over several seconds with ArI/PhI as the organic byproduct. The resulting manganese complex can be isolated by scraping microcrystalline residue from the sides of the vial after fast drying of the reaction mixture. The compound has been isolated in this way only in sparing amounts (the majority of the material remains in a mixture at the bottom of the vial) but decomposes in solution back to [(tpfc)Mn^{III}] over a period of 10 h at ambient temperature.

The resulting red-brown manganese complex can be assigned as the tosylimide of Mn(V), (tpfc)Mn^V=NTs (**2**) by spectroscopic comparison to the structurally characterized arylimido analogues.[4] The electronic spectrum of **2** shows distinctly different band structure from the Mn(III) starting material and compares well with the UV−vis of (tpfc)Mn^V=NMes (Mes = 2,4,6-trimethylphenyl), exhibiting two soret bands near 350 and 400 nm. The Q-band near 520 nm is less distinct and appears as a shoulder (Figure 1). Furthermore, the ESI mass spectrum of **2** exhibits a parent *m/z* peak of 861.9, which corresponds to (tpfc)Mn(N) as a result of N−S bond cleavage in the gas phase.

(9) (a) McLain, J. L.; Lee, J.; Groves, J. T. In *Biomimetic Oxidations Catalyzed by Transition Metal Complexes*; Meunier, B., Ed.; Imperial College Press: London, 2000; pp 91−169. (b) Meunier, B.; Bernadou, J. *Top. Catal.* **2002**, *21*, 47. (c) Watanabe, Y. In *The Porphyrin Handbook*; Kadish, K. M., Smith, K. M., Guilard, R., Eds.; Academic Press: New York, 2000; Vol. 4, pp 97−117.

(10) (a) Au, S.-M.; Huang, J.-S.; Yu, W.-Y.; Fung, W.-H.; Che, C.-M. *J. Am. Chem. Soc.* **1999**, *121*, 9120. (b) Leung, S. K.-Y.; Tsui, W.-M.; Huang, J.-S.; Che, C.-M.; Liang, J.-L.; Zhu, N. *J. Am. Chem. Soc.* **2005**, *127*, 16629. (c) Liang, J.-L.; Yuan, S.-X.; Huang, J.-S.; Che, C.-M. *J. Org. Chem.* **2004**, *69*, 3610. (d) Liang, J.-L.; Huang, J.-S.; Yu, X.-Q.; Zhu, N. Y.; Che, C.-M. *Chem. Eur. J.* **2002**, *8*, 1563. (e) Au, S.-M.; Fung, W.-H.; Cheng, M.-C.; Che, C.-M.; Peng, S.-M. *Chem. Commun.* **1997**, 1655.

(11) (a) Collman, J. P.; Chien, A. S.; Eberspacher, T. A.; Brauman, J. I. *J. Am. Chem. Soc.* **2000**, *122*, 11098. (b) Nam, W.; Choi, S. K.; Lim, M. H.; Rohde, J.-U.; Kim, I.; Kim, J.; Kim, C.; Que, L. Jr. *Angew. Chem. Int. Ed.* **2003**, *42*, 109. (c) Nam, W.; Lim, M. H.; Lee, H. J.; Kim, C. *J. Am. Chem. Soc.* **2000**, *122*, 6641.

(12) Wang, S. H.; Mandimutsira, B. S.; Todd, R.; Ramdhanie, B.; Fox, J. P.; Goldberg, D. P. *J. Am. Chem. Soc.* **2004**, *126*, 18.

(13) Edwards, N. Y.; Eikey, R. A.; Loring, M. I.; Abu-Omar, M. M. *Inorg. Chem.* **2005**, *44*, 3700.

(14) Abu-Omar, M. M.; Shields, C. E.; Edwards, N. Y.; Eikey, R. A. *Angew. Chem. Int. Ed.* **2005**, *44*, 6203.

(15) Macikenas, D.; Skrzypczak-Jankun, E.; Protasiewicz, J. D. *J. Am. Chem. Soc.* **1999**, *121*, 7164.

(16) (a) Turner, P; Gunter, M. J. *Inorg. Chem.* **1994**, *33*, 1406. (b) Groves, J. T.; Haushalter, R. C.; Nakamura, M.; Nemo, T. E.; Evans, B. J. *J. Am. Chem. Soc.* **1981**, *103*, 2884.

(17) Bendix, J.; Gray, H. B.; Golubkov, G.; Gross, Z. *Chem. Commun.* **2000**, 1957.

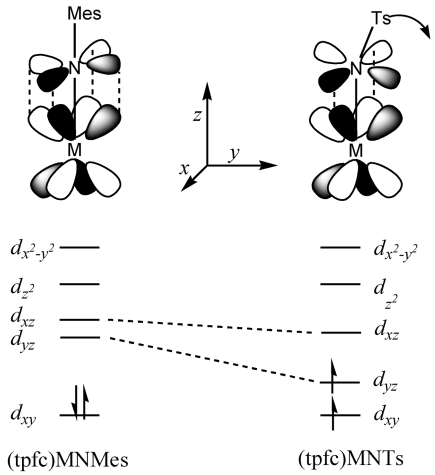

Figure 2. Geometric effects on electronic structure of d^2 metals with linear terminal mesitylimido (left) and bent terminal tosylimido (right) under C_s symmetry. The d_{xz} and d_{yz} orbitals are lowered in energy in the tosylimido complex due to weaker overall π-donation by the tosylimido ligand in comparison to mesitylimido. The bend at nitrogen in the tosylimido complex further lowers the energy of the d_{yz} orbital by disrupting the π-overlap between the nitrogen p_y and metal d_{yz} orbitals, resulting in a high-spin complex.

Even though the manganese tosylimide was problematic in affording large enough single crystals for X-ray analysis, the structure of (tpfc)Cr^V═NTs, prepared from the reaction of ArI═NTs and (tpfc)$Cr^{III}(py)_2$, was solved (see Supporting Information).

Unlike the diamagnetic (tpfc)Mn^V═NMes, **2** is paramagnetic, exhibiting broad ^{19}F signals, and no visible resonances in the ^{1}H NMR spectrum are observed. Instead, the diamagnetic ^{1}H and ^{19}F NMR signals belonging to (tpfc)Mn^V═O (**5**) are observed in small amounts as a result of protolysis by H_2O.[18] Magnetic susceptibility measurements (Evans method) demonstrate a μ_{eff} of 3.24 BM, most consistent with an $S = 1$ complex. While this spin state differs from the $S = 0$ (tpfc)Mn^V═NMes, it is consistent with a terminal imido with poor π-donation, which lowers the energy of the d_{xz} and d_{yz} orbitals in comparison to NMes. Additional electronic structure information can be inferred from the structure of (tpfc)Cr^V═NTs in the Supporting Information. While the Cr—N terminal imido bond length (1.65 Å) is comparable to that of the known (tpfc)Cr═NMes and (tpfc)Mn═NMes, the nitrogen atom of the tosylimido exhibits a bond angle of 150.7°, while the mesitylimidos are linear at nitrogen. This bend at nitrogen suggests at most a single strong N—Cr π-bond, perpendicular to the Cr—N—S plane. Assuming structural similarity for the manganese complex, the absence of the second π-bond would lower the energy of the corresponding d orbital, resulting in the observed triplet state (Figure 2). This trend has been observed by Odom and co-workers in a series of bis-imido metal complexes of the chromium group. Using NMR shielding and DFT arguments, this study concluded that a bend at nitrogen coincides with a more shielded (hence more nitrene-like) imide ligand, which is an overall poorer electron donor than a linear imide.[19] The $S = 1$ spin state has been observed for porphyrinato manganese(V) oxo by magnetic measurements.[20] It should be noted that the observed value of μ_{eff} (3.24 BM) is slightly higher than the theoretical value of 2.83 BM due to some inevitable decomposition of **2** back to the higher magnetic moment **1**. When **2** is allowed to decompose back to green **1**, the expected spin state ($S = 2$, $\mu_{eff} = 4.72$ BM) of Mn^{III}(tpfc) is observed by magnetic measurement (Evans method). $S = 2$ is observed for **1** regardless of axial ligation.[21]

In addition to water, solvents such as toluene and acetonitrile result in decomposition of **2**, though at much slower rate, and via HAT instead of protolysis. The organic byproduct from decomposition of **2** is H_2NTs. Even though complex **2** lasts hours in dry benzene, it still decomposes back to Mn^{III}, **1**, through pathways that we cannot fully account for at this time. Small amounts of adventitious moisture that cannot be avoided could be responsible for the slow decomposition in benzene. However, we did not observe formation of (tpfc)$Mn^V(N)^{3d}$ or disubstituted diazene upon decomposition of **2** (NMR, UV—vis, and GC). The absence of the latter suggests that this system is not amenable to bimolecular coupling of the imido group. Formation and decomposition of **2** is summarized in Scheme 1.

The EPR spectrum of **2** generated in situ exhibits a number of assignable signals, suggesting some degree of speciation in solution.[22] The concentration of these extra species is most likely very minor, given the comparability of the absorption spectrum of **2** to that of (tpfc)Mn^V═NMes, which suggests that the majority of manganese in solution is in the form of terminal imido. Among the EPR signals observed is a broad feature at $g = 4$, which we assign to **2**. While no comparable signal has been reported for a high-spin manganese(V) porphyrin or corrole complex to our knowledge, this signal is consistent with a spin forbidden transition $\Delta m_s = \pm 2$ for a triplet-state complex and thus a weak signal.[22d,e] Upon addition of H_2O to form diamagnetic (tpfc)Mn═O, this feature disappears. In summary, characterization of complex **2** is consistent with high-spin (tpfc)-

(18) (a) Gross, Z.; Golubkov, G.; Simkhovich, L. *Angew. Chem. Int. Ed.* **2000**, *39* (22), 4045. (b) Addition of H_2O to a red-brown solution of **2** results in formation of a red solution with diamagnetic β-pyrrole ^{1}H NMR signals belonging to (tpfc)Mn^V═O, concurrently with $TsNH_2$, the two compounds appearing in a 1:1 ratio. We have confirmed the identity of this hydrolysis product by comparison of the electronic absorption and ^{1}H NMR spectra to the manganese-oxo complex generated by reaction of **1** with PhIO. The electronic absorption and ^{1}H NMR spectra are identical whether generated directly or by hydrolysis of **2**, although the behavior of this manganese-oxo is different in our hands than reported by Gross et al,[18a] which indicates that the manganese oxo lasts minutes at millimolar concentrations (hours in our hands), and hours at micromolar concentrations (days in our hands). Additionally, this report claims that cold temperatures (−75 °C) are necessary to observe broad *b*-pyrrole signatures, while we are able to obtain a well-resolved spectrum with sharp signatures at room temperature. Lastly, our electronic absorption spectrum differs substantially from Gross's reported spectrum for isolated (tpfc)Mn^V═O, but matches the spectrum he reports for (tpfc)Mn^V═O generated in situ (spectra are provided in the Supporting Information).

(19) Ciszewski, J. T.; Harrison, J. F.; Odom, A. L. *Inorg. Chem.* **2004**, *43*, 3605.

(20) Groves, J. T.; Kruper, W. J.; Haushalter, R. C. *J. Am. Chem. Soc.* **1980**, *102*, 6375.

(21) The $S = 2$ spin state is observed when there is no axial ligation in solution, as well as when the complex exists as a pyridine adduct based on magnetic measurement by Evans' method ($\mu_{eff} = 5.28$ BM, see Supporting Information).

(22) (a) A broad signature near $g = 8$ is consistent with residual Mn(III).[22b] As manganese(III) porphyrin complexes are normally silent by X-band EPR,[17] it is unclear whether this signal results from **1** or from trace Mn^{3+} in another ligand environment. A hyperfine feature present at 4.3 is comparable to those for Mn^{2+} ion in a high zero-field-splitting environment, such as in the manganese superoxide dismutases.[22c] This feature remains after addition of H_2O. A broad signal at $g = 4$ is assigned to **2**.[22d,e] An intense 16-line feature at $g = 2.0$ is consistent with a $S = 1/2$ manganese dimer.[22e] This signal appears as a result of hydrolysis of **2** by H_2O and is believed to be a minor byproduct accompanying the formation of the major diamagnetic (tpfc)Mn^V═O product observed by electronic absorption spectroscopy and ^{1}H and ^{19}F NMR. See Supporting Information for spectra. (b) Talsi, E. P.; Bryliakov, K. P. *Mendeleev Commun.* **2004**, *3*, 111. (c) Hsieh, Y.; Guan, Y.; Tu, C.; Bratt, P. J.; Angerhofer, A.; Lepock, J. R.; Hickey, M. J.; Tainer, J. A.; Nick, H. S.; Silverman, D. N. *Biochemistry.* **1998**, *37*, 4731. (d) Eisch, J. J.; Gitua, J. N.; Doetschman, D. C. *Eur J. Inorg. Chem.* **1994**, *33*, 1406. (e) Van der Waals, J. H.; de Groot, M. S. *J Chim. Phys.* **1964**, 1643. (f) Chen, H.; Tagore, R.; Das, S.; Incarvito, C.; Faller, J. W.; Crabtree, R. H; Brudvig, G. W. *Inorg. Chem.* **2005**, *44*, 7661.

Scheme 1. Formation and Decomposition of Mn^V Tosylimido **2**

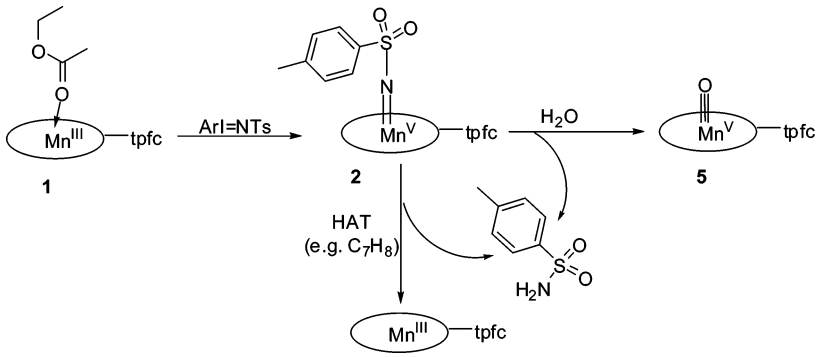

Mn^V═NTs. Detailed spectroscopic characterization of **2** by parallel-mode EPR and X-ray absorption spectroscopy will be the subject of another report.

Identity of the Active Manganese Catalyst Responsible for Group Transfer. To our surprise the manganese(V) tosylimide **2** does not transfer [NTs] to styrene to give aziridine. With excess styrene, the red-brown solution of **2** turns green and H_2NTs along with ArI are detected by GC; however, no aziridine is produced. Under these stoichiometric conditions we have not been able to identify any organic products from styrene. Purification of styrene via distillation to remove potentially reactive impurities did not change the outcome. The one affirmative conclusion we can ascertain from this reaction is that (tpfc)Mn^V═NTs does not transfer [NTs] to styrene to give aziridine. This finding may not be so surprising if we consider the recent studies of Newcomb and co-workers on the reaction kinetics of metal-oxo species containing porphyrin and corrole ancillary ligand.[23] In these studies, photochemically generated (tpfc)Mn^V═O was found to be $\sim 10^5$ less reactive as an oxygen atom transfer species toward cyclooctene than its porphyrin analogue (tpfp)Mn^V═O (tpfp = 5,10,15,20-tetrakis(pentafluorophenyl)porphyrin).

Further confirmation that complex **2** is not the active form of the catalyst came from steady-state kinetics. Oxidative formation of **2** (vide infra) is fast as compared to reduction of **2** back to **1.** Nevertheless, under steady-state conditions, formation of aziridine (followed by ^{1}H NMR) was zero-order in [styrene] (Figure 3). Also the rate of aziridine formation (initial rate method) exhibited first-order dependence on the initial concentration of ArINTs. Thus, formation of the oxidizing species is rate-determining under catalytic steady-state conditions.

We turned first to the mechanism proposed by Nam and Que[11b] for oxidation with iron porphyrin and PhI═O, namely, a metal−oxidant adduct as the active species (eq 1). One experimental finding we already had against this mechanism is that the reaction between ArI═NTs and **1** to give **2** is not reversible. To probe this further, we monitored the catalytic reaction starting with a solution of (tpfc)Mn^{III} (10 mol %) and styrene and adding ArI═NTs last. We looked in the initial stages to see if there is a burst of product that would result from the adduct (tpfc)Mn^{III}(ArI═NTs) prior to formation of complex **2**. The result was negative. We also looked for an induction period if we started with the manganese tosylimide **2** as the starting catalyst. The results were again negative. In conclusion, irrespective of the starting form of the catalyst (Mn^{III} vs Mn^V) the kinetics profiles for aziridine formation were identical.

Next we considered the manganese−oxo complex resulting from hydrolysis of **2** (vide supra) as the active catalyst. When the aziridination of styrene is carried out in solvents that have not been dried to remove water, the reaction mixture is bright red (from (tpfc)MnO) instead of red-brown (from (tpfc)MnNTs), and no aziridine is formed. Furthermore, when (tpfc)MnO is generated directly from **1** and PhIO in dry solvent and subsequently added to a mixture of styrene and PhINTs, minimal aziridination is observed. While (tpfc)MnO has been reported to catalyze epoxidation of styrene,[18a] we did not observe stoichiometric oxidation of styrene by (tpfc)MnO to form styrene oxide. From these observations, we conclude that the manganese oxo complex **5** is not the catalyst responsible for group transfer.

Finally we considered the "third oxidant" suggested by Goldberg and co-workers.[12] Here the "third oxidant" could be an iodoimine adduct of **2**, (tpfc)Mn^V(NTs)(ArI═NTs) (**4**), or a transient Mn(VII) bisimido, (tpfc)$Mn^{VII}(NTs)_2$ (**6**). To address the validity of either pathway we turned to labeling experiments. We prepared the *tert*-butyl analogue of ArI═NTs with a *p*-*tert*-butyl substituent instead of *p*-methyl on the tosylimine (Scheme 2). We first established that this reagent (ArI═NTs^{tBu}) indeed forms aziridine with styrene in the presence of catalyst **1** at a comparable rate to that observed for ArI═NTs, isolated the aziridine, and obtained its GC retention time (15.2 min), which is clearly distinguishable from the aziridine with the parent *p*-tolylsulfonylimine (11.6 min). The expectations as detailed in Scheme 2 are as follows: If the "third oxidant" is an adduct

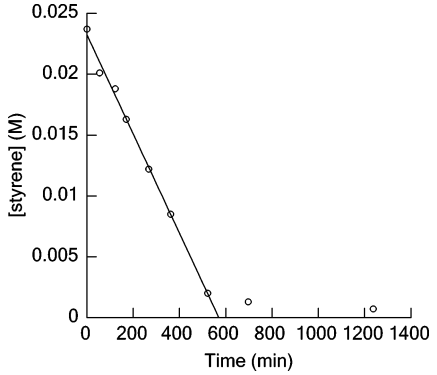

Figure 3. Steady-state kinetics for catalytic aziridination. 2 equiv of solid ArINTs were stirred in a 24 mM solution of styrene with 1.5 mol % **1** as catalyst (0.39 mM). Experimental data are represented by points. The solid line represents the theoretical linear fit to the linear region: slope = $(-4.0 \pm 0.1) \times 10^{-5}$ M min^{-1}; $R = 0.998$.

(23) (a) Zhang, R.; Newcomb, M. *J. Am. Chem. Soc.* **2003**, *125*, 12418. (b) Zhang, R.; Horner, J. H.; Newcomb, M. *J. Am. Chem. Soc.* **2005**, *127*, 6573. (c) Zhang, R.; Chandrasena, R. E. P.; Martinez, E., II; Horner, J. H.; Newcomb, M. *Org. Lett.* **2005**, *7*, 1193. (d) Harischandra, D. N.; Zhang, R.; Newcomb, M. *J. Am. Chem. Soc.* **2005**, *127*, 13776.

Scheme 2. Potential Outcomes of the Double-Labeling Experiment for Different Aziridination Mechanisms

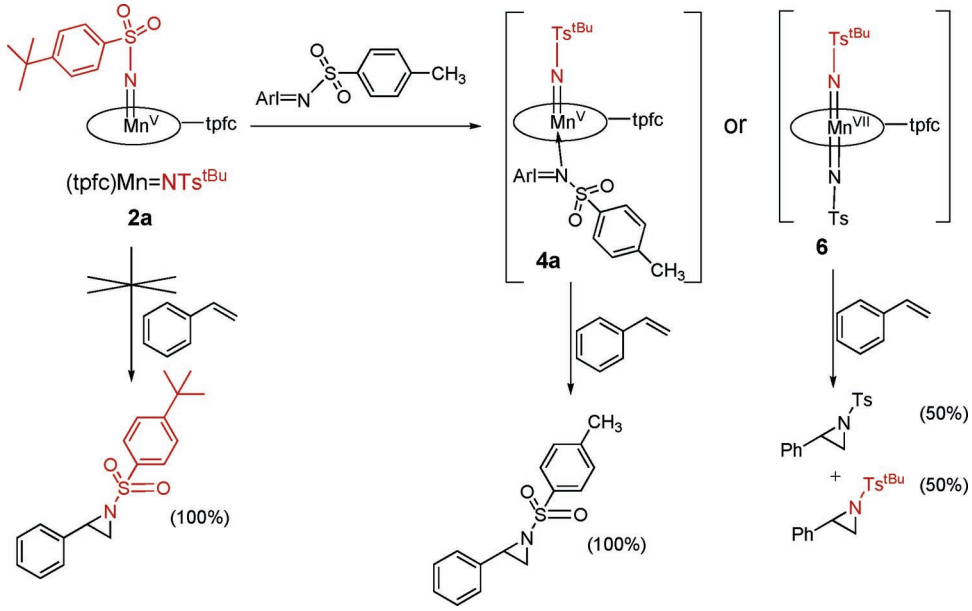

(**4**) of Mn(V) imide, only one aziridine would be formed. If the "third oxidant" is a transient Mn(VII) bisimido (**6**), 50:50 mixture of two possible aziridines will be obtained.

We performed this double labeling experiment twice. In the first we generated complex **2a**, (tpfc)Mn^{V}=NTs^{tBu} and added 1 equiv of ArI=NTs concurrently with 1 equiv of styrene. The reaction product was analyzed by GC. The ratio of the two aziridines NTs:NTs^{tBu} = 100:1 (Figure 4). In the second experiment, we generated complex **2** and added 1 equiv of ArI=NTs^{tBu} concurrently with 1 equiv of styrene. The ratio of the two aziridines NTs:NTs^{tBu} = 1:10. These findings provide unambiguous evidence that the group transfer catalyst is an adduct analogous to Goldberg's "third oxidant" as illustrated in Scheme 2, which also accounts for zero-order dependence on [styrene] and lack of aziridine formation from Mn(V) imido **2**. The presence of Ts^{tBu}NH$_2$ in the GC trace is because the reaction was allowed to stand until the solution turned green, that is all the Mn(V) imido reverted to manganese(III). The smaller amount of TsNH$_2$ is likely due to some decomposition of ArI=NTs under these dilute (mM) stoichiometric conditions. Nevertheless, more than 70% of the initial styrene was converted to azirdine. As for the difference of a factor of 10 between the two double-labeling experiments, we attribute this to the limited precision of the experiment, precisely, in measuring an exact equivalent of iodoimine relative to the starting Mn(III) complex (**1**) at this scale. Furthermore, the reactivity of ArI=NTs^{tBu} is quite comparable to that of ArI=NTs under steady-state conditions and thus would not account for the observed difference. In summary, a difference of 10 between the yields of the two possible aziridines is sufficient to decisively discriminate between the two possible mechanisms.

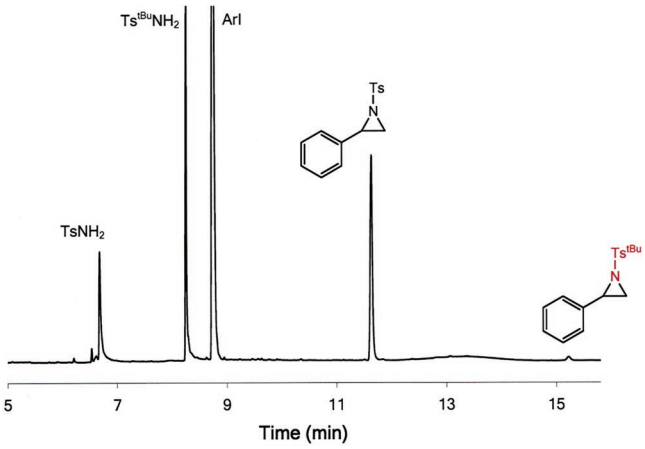

Figure 4. Gas chromatogram from the labeling competition experiment between transfer of NTs^{tBu} vs NTs to olefin. In this experiment, to (tpfc)-MnNTs^{tBu} was added 1 equiv of ArINTs and styrene concurrently. The predominant signal at 11.6 is indicative of aziridination by NTs, while the small signal at 15.2 is indicative of the minor aziridination by NTs^{tBu}. Other signals appearing in the trace areTsNH$_2$ at 6.7 min, Ts^{tBu}NH$_2$ at 8.2 min, and ArI at 8.7 min.

Probing Electronic Effects on Group Transfer to Alkenes. Since the rate-determining step under steady-state kinetics does not involve the alkene, styrene, information on the group transfer step cannot be obtained from direct kinetic measurements. However, measurement of product ratios resulting from two styrene substrates that compete for the active intermediate would be directly proportional to the ratio of the substrates' rate constants as long as the oxidant is limiting and the styrene substrates are used in excess (Scheme 3 and eq 3). Three styrene

Scheme 3. Ratio of Rate Constants from Ratio of Products under Competition Kinetics

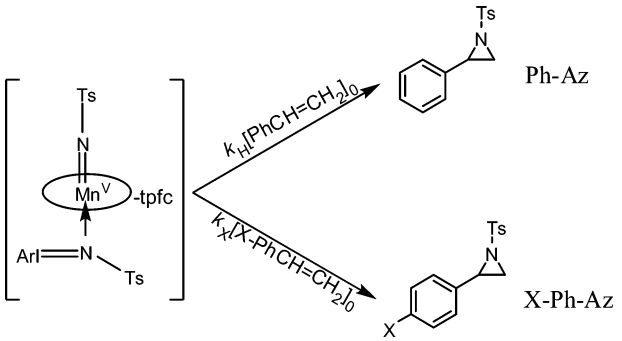

$$\frac{[X-Ph-Az]_\infty}{[Ph-Az]_\infty} = \frac{k_X[X-PhCH=CH_2]_0}{k_H[PhCH=CH_2]_0} \quad (3)$$

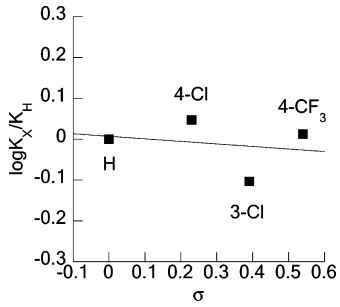

Figure 5. Hammett plot from competition between substituted styrenes. 0.1 equiv of ArINTs was stirred with a 1:1 mixture of substituted olefin and styrene (20 mM for each) and 1.5% catalyst **1** (0.29 mM). Ratio of rate constants was calculated based on the ratio of aziridine products. Points represent experimental data except for the origin point set for styrene. The solid line represents the theoretical linear fit: slope = −0.06 ± 0.2.

substrates (4-Cl, 3-Cl, and 4-CF_3-styrene) were selected for competition with styrene. The aziridine product ratios for each competition experiment were determined by GC and were found to be quite close to unity in each instant. A Hammett plot of $\log(k_x/k_H)$, calculated from the aziridine product ratio per eq 3, versus the Hammett substituent constant σ is shown in Figure 5. There is no significant electronic effect for the group transfer step. The reaction constant ρ is essentially zero (−0.06 ± 0.2). This observation is consistent with a nonpolar transition state that is unaffected by electronic substitutents on the aryl ring.[24] The most likely scenario is a radical-type mechanism in which the olefin approaches from the unhindered β-carbon to form an intermediate nitrogen and carbon radical cage, followed by rapid recombination to afford the product (eq 4). This mechanism has been invoked recently for aziridination in one report by ruthenium and in another for manganese and iron porphyrins based upon secondary isotope effects and product stereochemical arguments, respectively.[10a,25] The mechanism in eq 4 is also consistent with the observation that **1** is an effective catalyst for α-disubstituted styrenes but not for β-substituted styrene:

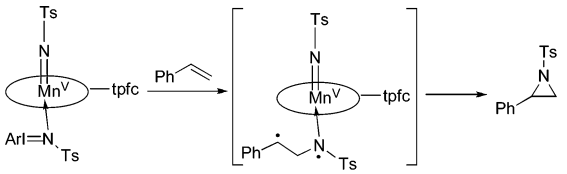

(4)

Kinetics and Mechanism of Manganese(V) Imido Formation. While PhI═NTs is the common nitrene source in aziridination reactions,[1a] its use in quantitative kinetics is hampered by its lack of solubility and polymeric nature. The development of molecular analogues such as ArI═NTs (Ar = 2-(*tert*-butylsulfonyl)benzene)[15] that are soluble makes kinetic studies feasible. We studied the kinetics of the reaction of ArI═NTs with (tpfc)Mn(EtOAc) using stopped-flow spectroscopy. Under pseudo-first-order conditions (limiting manganese corrole and excess ArI═NTs) disappearance of manganese(III) complex **1** monitored at λ = 600 nm is first order in **1** (Figure 6) and the plot of k_ψ (pseudo-first-order rate constants) versus [ArI═NTs]

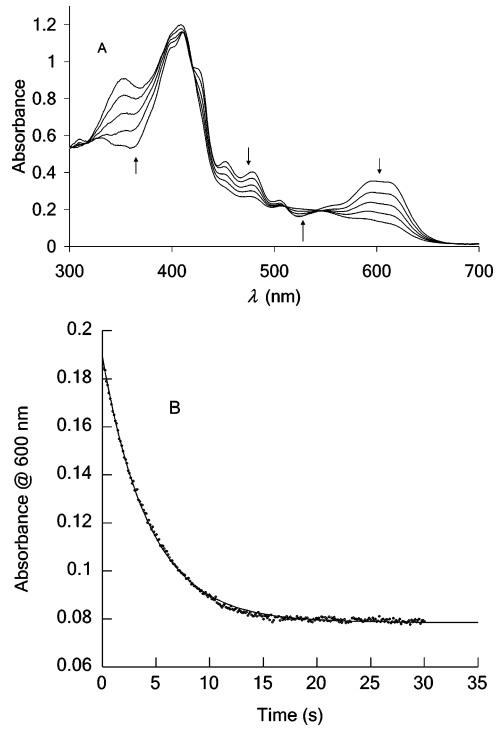

Figure 6. (A) Stack UV−vis plot showing isosbestic conversion of **1** to **2** by titration with ArINTs. (B) A typical kinetic trace for the formation of **2** from **1** and excess ArINTs monitored using stopped-flow spectroscopy at 600 nm (data designated by points, fit designated by solid line). Conditions: T = 24 °C, [**1**] = 2.53 × 10^{-5} M, and [ArINTs] = 6.3 × 10^{-4} M.

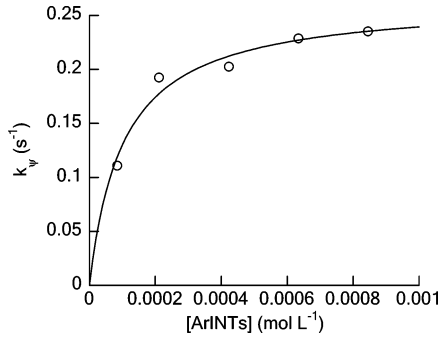

Figure 7. Plot of pseudo-first-order rate constant vs [ArINTs] exhibiting saturation kinetics. Points represent experimental data. Solid line represents theoretical fit. k_4 = 0.26 ± 0.07 s^{-1} and K_3 = (10 ± 2) × 10^3 L mol^{-1} at 24.0 ± 0.2 °C, R = 0.98.

(Figure 7) features kinetic saturation in oxidant. Two kinetically indistinguishable mechanisms can account for the observed rate law (Scheme 4 and eqs 5 and 6). The rate law for mechanism A in Scheme 4 based on the steady-state approximation is given in eq 5. This pathway (Scheme 4A) is discounted on the basis that negligible inhibition is observed by added ethyl acetate. At ethyl acetate concentrations comparable to those in our kinetic runs, inhibition is not observed. A 2000-fold excess of EtOAc is required to decrease the reaction rate by a meager 10%. Additionally, we have UV−vis evidence to suggest that the predominant manganese species in solution is the 4-coordinate free metal corrole, not the 5-coordinate EtOAc adduct. In benzene, titration of **1** with EtOAc does lead to a change in the UV−vis spectrum, but the equilibrium constant of 76 calculated by the absorbance change with respect to ethyl acetate concentration suggests that, in a typical 5 × 10^{-5} M solution

(24) (a) Dinçtürk, S.; Jackson, R. A. *J. Chem. Soc. Perkin Trans. 2.* **1981**, 1127. (b) Walling, C.; Briggs, E. R.; Wolfstirn, K. B.; Mayo, F. R. *J. Am. Chem. Soc.* **1948**, *70*, 1537. (c) Rybtchinski, B.; Vigalok, A.; Ben-David, Y.; Milstein, D. *J. Am. Chem. Soc.* **1996**, *118*, 12406.
(25) Simonato, J.-P.; Pécaut, J.; Scheidt, R.; Marchon, J.-C. *Chem. Commun.* **1999**, 989.

Scheme 4. Possible Mechanisms for Formation of **2**

A. $(tpfc)Mn(EtOAc) \underset{k_{-1}}{\overset{k_1}{\rightleftharpoons}} [(tpfc)Mn] + EtOAc$

$[(tpfc)Mn] + ArI{=}NTs \xrightarrow{k_2} (tpfc)Mn^{V}{=}NTs + ArI$

B. $[(tpfc)Mn] + ArI{=}NTs \underset{k_{-3}}{\overset{k_3}{\rightleftharpoons}} [(tpfc)Mn(ArINTs)]$

$[(tpfc)Mn(ArINTs)] \xrightarrow{k_4} (tpfc)Mn^{V}{=}NTs + ArI$

$$\frac{d[(tpfc)Mn{=}NTs]}{dt} = k_{\psi}[(tpfc)Mn(EtOAc)] = \frac{k_1k_2[(tpfc)Mn(EtOAc)][ArI{=}NTs]}{k_{-1}[EtOAc] + k_2[ArI{=}NTs]} \quad (5)$$

$$\frac{d[(tpfc)Mn{=}NTs]}{dt} = k_{\psi}[Mn]_T = \frac{K_3k_4[Mn]_T[ArI{=}NTs]}{1 + K_3[ArI{=}NTs]} \quad (6)$$

of **1**·EtOAc used in catalysis, **1** is 99.6% unligated. Additionally, the UV−vis spectrum of crystalline **1**·EtOAc dissolved in benzene is identical to the spectrum of **1** in which EtOAc has been removed from the solid by sublimation. These results provide strong evidence that **1** does not exist as a 5-coordinate ethyl acetate adduct in benzene solution.

Given the above results, reversible formation of iodoimine adduct $(tpfc)Mn^{III}(ArI{=}NTs)$, **3**, followed by unimolecular oxidation of Mn(III) to Mn(V) (Scheme 4B and eq 6) is the favored mechanism. Fitting the experimental data in Figure 7 to the rate law based on the prior equilibrium approximation (eq 6) yields $k_4 = 0.26 \pm 0.07\ s^{-1}$ and an equilibrium constant for formation of **3** $K_3 = (10 \pm 2) \times 10^3\ L\ mol^{-1}$ at 24.0 ± 0.2 °C.

It is worth noting that the reaction of **1** with ArI═NTs to give complex **2** is not reversible. The addition of ArI (100 equiv) to a solution of **2** does not result in reversion to **1** according to Le Chatelier's principle. This is in contrast to a reported evidence that the reaction of iron porphyrin with PhI═O is reversible.[11b]

Catalytic Group Transfer to Olefins. The classical aziridination reagent PhI═NTs was introduced as a nitrene source for group transfer reactions to C−H and C═C bonds catalyzed by heme enzymes and biomimetic metalloporphyrins.[26] It has also been employed with chiral transition metal catalysts in asymmetric aziridination.[1a,27] A major drawback for the overwhelming majority of known catalysts is the requirement of excess olefin (10- to 100-fold relative to PhI═NTs). For example, iron corroles in the oxidation states +3 and +4 catalyze styrene aziridination with catalyst:PhI═NTs:styrene = 1:100:10 000.[28a] Recently, Zhang and co-workers have reported first an iron and then a cobalt porphyrin complex, which have achieved aziridination catalysis on a wide array of olefins with a limiting olefin (olefin:nitrene ratio of 1:2); moderate (5−10 mol %) catalyst loadings are necessary to achieve reasonable to good yields.[28b,c] **1** catalyzes the aziridination of styrene substrates effectively in benzene with low catalyst loading (1−2 mol %) and without requiring excess olefin (Table 1). Aziridine

(26) (a) Breslow, R.; Gellman, S. H. *J. Chem. Soc. Chem. Commun.* **1982**, 1400. (b) Mansuy, D.; Mahy, J.-P.; Dureault, A.; Bedi, G.; Battoni, P. *J. Chem. Soc. Chem. Commun.* **1984**, 1161.
(27) Llewellyn, D. B.; Adamson, D; Arndtsen, B. A. *Org. Lett.* **2000**, *2*, 4165.
(28) (a) Simkhavich, L.; Gross, Z. *Tetrahedron Lett.* **2001**, *42*, 8089. (b) Vyas, R; Gao, G.-Y.; Harden, J. D.; Zhang, P. *Org. Lett.* **2004**, *6*, 1907. (c) Gao, G.-Y.; Harden, J. D.; Zhang, P. *Org. Lett.* **2005**, *7*, 3191.

Table 1. Catalytic Aziridination of Olefins[a]

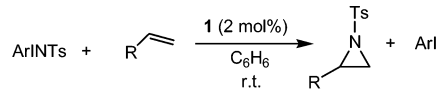

Entry	R	% Yield[b]
1	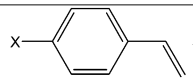 X = Cl, OMe, H	> 98 (X=H 67, X=Cl 50)[c]
2	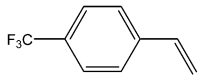	85
3	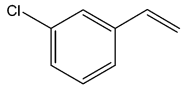	> 98
4	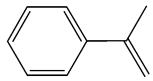	85

[a] Conditions: 2 equiv of solid ArINTs was stirred with styrene (20 mM) and 2 mol % **1** (0.4 mM) in benzene for 48 h. [b] Yields were determined by integration of methine and methylene aziridine ^1H NMR signals against an internal standard ($(SiEt_3)_2O$). [c] Values in parentheses represent isolated yields. Isolated yields were lower due to overlapping of the aziridine and ArI bands from the silica column.

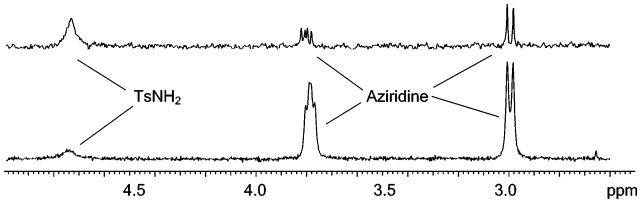

Figure 8. ^1H NMR spectral region showing aziridine methine and methylene signals as well as $TsNH_2$ N−H signals from in situ reactions. Conversion to aziridine is optimized in benzene (bottom), while formation of $TsNH_2$ from HAT dominates in toluene (top).

yields were determined by ^1H NMR spectroscopy. Even though complex **1** is an effective catalyst for aryl olefins, it does not catalyze aziridination of aliphatic alkenes such as 1-hexene and cyclohexene or olefins with β-subtitution such as *cis*- and *trans*-β-methyl styrene or *cis*- and *trans*-stilbene.

The reaction between ArI═NTs and **1** is much faster than the reduction of **2** back to **1**. Thus, under steady-state conditions the major form of the catalyst is $(tpfc)Mn^{V}{=}NTs$, **2**, and the color of the reaction solution is red-brown throughout the reaction until all substrates are consumed at which time the catalyst reverts to the green Mn(III) (given that ArI═NTs is not used in large excess). When toluene was used as solvent, we noted lowered aziridine yields accompanied by substantial $TsNH_2$ byproduct formation. A comparison of the catalytic reaction with styrene in the two solvents (benzene versus toluene) is shown in Figure 8. We attribute this to hydrogen atom transfer (HAT) from toluene. The ability of **2** to effect hydrogen abstraction from benzylic hydrogens is demonstrated by the HAT reaction of complex **2** with 9,10-dihydroanthracene (DHA) to give anthracene. The reaction displays a primary kinetic isotope effect $k_H/k_D = 3.5$ for DHA versus deutero-DHA. The details of HAT reaction with complex **2** will be taken up in a future paper. However, we cannot exclude the possibility that another form of manganese corrole that is present in small concentration under catalytic conditions is more effective than

complex **2** at HAT reactions, such as the "third oxidant" **4** suggested above for the aziridination reaction. Recently the groups of Borovik and Holland have reported on HAT from putative Fe(IV) imido intermediates.[29]

Conclusion

The manganese(V) tosylimide with a corrole auxiliary ligand has been synthesized and spectroscopically characterized. The reaction of (tpfc)Mn^{III}(EtOAc) and ArI═NTs proceeds rapidly on stopped-flow time scale, and the experimental rate law is in agreement with a mechanism that involves iodoimine adduct formation, (tpfc)Mn^{III}(ArI═NTs), in route to the manganese(V) imido product, (tpfc)Mn^{V}═NTs. While (tpfc)Mn serves as an effective catalyst for aziridination of styrene substrates without requiring excess olefin, the imido complex (tpfc)Mn^{V}═NTs is not the active intermediate. Labeling experiments demonstrate unambiguously that the active group transfer catalyst is an adduct of Mn(V), (tpfc)Mn^{V}(NTs)(ArI═NTs).

Experimental Section

General. All operations were carried out under inert atmosphere using standard glovebox and Schlenk line techniques[30] except where otherwise noted. Benzene, toluene, and *n*-pentane were distilled from sodium benzophenone ketyl; acetonitrile and pyrrole were distilled from CaH_2; CH_2Cl_2 was obtained from an Anhydrous Engineering solvent purification system. Solvents were degassed and stored over activated 4-Å molecular sieves in a glovebox for 24 h prior to use. NMR solvents were purchased from Cambridge Isotope Laboratories. Those used for aziridination kinetics and for observation of **2** were stored over activated 4-Å molecular sieves for 24 h prior to use. $Ts^{tBu}NH_2$ was purchased from Oakwood Products, Inc. Olefins were purchased from Aldrich (X-styrene (X═H, 4-CF_3, 4-Cl, 3-Cl), α-methylstyrene, *cis*- and *trans*-stilbene, and *trans*-*β*-methylstyrene) and TCI (*cis*-*β*-methyl styrene). All purchased chemicals were used as obtained from the manufacturers unless specified otherwise.

UV−vis spectra were recorded on a Shimadzu UV-2501PC scanning spectrophotometer. NMR spectra were obtained on Inova/Varian 300 MHz spectrometers. Gas chromatography was carried out on an Agilent Technologies 6890N Network GC System with a J&W Scientific DB-5 capilary column. Oven temperature was ramped from 70 to 150 °C at 25 °C/min, then from 150 to 230 at 15 °X/min in constant flow mode at 2.5 mL/min. Kinetics were performed using an Applied Photophysics SX.18MV stopped-flow analyzer. Data were fit to theoretical curves using KaleidaGraph.

Synthesis: 2-(*tert*-Butylsulfonyl)iodobenzene (ArI) and **2-(*tert*-butylsulfonyl)(*p*-toluenesulfonyliminoiodo)benzene (ArINTs)** were prepared according to the method of Macikenas et al.[15]

***p*-Toluenesulfonyliminoiodobenzene (PhINTs)** was prepared according to the method of Heuss et al.[31]

5,10,15-Tris(pentafluorophenyl)corrole ((tpfc)H_3). A facile synthesis of H_3(tpfc) has been described by Gross et al.[32] We have been unable to reproduce the yields described and have therefore adopted the following revised protocol to maximize product yield: to 15 g of Brockmann I alumina with enough dry CH_2Cl_2 to cover the alumina, 5.04 g (75 mmol) of pyrrole was added with slow stirring, followed by 14.7 g (75 mmol) of pentafluorobenzaldehyde. The reaction mixture was heated at 60 °C open to atmosphere to afford a gradual color change to brown. Once all solvent had evaporated, the mixture was heated for an additional 4 h and then cooled at room temperature for 12 h. The solid was dissolved in 100 mL of CH_2Cl_2 and filtered to remove alumina; 8.52 g (37.5 mmol) of solid 2,3-dichloro-5,6-dicyano-1,4-benzoquinone was added slowly (to avoid overboiling) with stirring to afford a color change to black. This solution was stirred for 8 h and separated on a silica column with 1:1 CH_2Cl_2:hexanes as eluant. The location of product corrole on the column is apparent by its red fluorescence under long-wave UV light. The solvent was removed from the product-containing fraction in vacuo, and the product was separated on a second column of alumina with CH_2Cl_2:hexanes as eluant. A 1:2 mixture was used to elute the initial fractions; a 1:1 mixture was then substituted until the product began eluting, and a 2:1 mixture was used to encourage elution of the remainder of the product. The solvent was removed in vacuo, and the solid was recrystallized from CH_2Cl_2 and hexanes to give 0.59 g of H_3(tpfc) (0.72 mmol, 4.0%) as purple-gray crystals.

Mn(tpfc)EtOAc·EtOAc (1) was prepared according to a modified procedure of Gross et al.[18a] Before chromatographic separation, the dried reaction mixture was heated gently under vacuum for 30 min to remove all traces of DMF. The crystalline material obtained after chromatography is suitable for use as a reagent or catalyst but can be further purified by recrystallization from ethyl acetate/heptane (82% recovery). UV−vis (C_6H_6): λ_{max} [nm] (log ϵ) = 400 (4.64), 409 (4.67), 422 (4.60), 450 (4.28), 478 (4.21), 504 (4.02), 593 (4.16), 611 (4.16). Anal. Calcd for $C_{41}H_{16}F_{15}MnN_4O_2{\cdot}C_4H_8O_2$: C, 52.75; H, 2.26; N, 5.47. Found: C, 52.71; H, 2.26; N, 5.53. MS (MALDI) *m*/*z*: 847.73 (theory = 848.426 for Mn(tpfc)).

2-(*tert*-Butylsulfonyl)(*p*-(*tert*-butylbenzene)sulfonyliminoiodo)-benzene (ArINTs^{tBu}) was prepared according to a modified procedure for the preparation of ArINTs.[15] To a stirred yellow solution of ArI-$(OAc)_2$[15] (3.00 g, 6.74 mmol) in MeOH (50 mL), a solution of KOH (1.5 g, 27 mmol) in MeOH (50 mL) was added, followed immediately by a solution of $Ts^{tBu}NH_2$ (1.45 g, 6.80 mmol) in MeOH (50 mL) under atmospheric conditions. The resulting cream-colored suspension was stirred for 4 h, poured into 1 L of ice, and chilled at 4 °C for 10 h. The mixture was filtered to give 0.922 g of cream-colored solid, and the filtrate was saved. The residue was washed with 8 mL of C_6H_6 for 30 min and filtered to give 0.421 g of ArINTs^{tBu}. The initial filtrate was evaporated in vacuo by 20 mL and chilled at 4 °C for 10 h to give more cream-colored solid, which was filtered and washed with benzene to give 0.559 g of more ArINTs^{tBu}. Total yield: 0.980 g, 28%. ^{1}H NMR (CD_3CN) δ: 1.23 (s, 9H, Ts-^{t}Bu), 1.38 (s, 9H, $SO_2{}^t$Bu), 7.37 (dd, 2H, Ts-*m*-H), 7.67 (m, 2H, Ar−H 3- and 4-position), 7.11 (dd, 2H, Ts-*o*-H), 7.80 (ddd, 1H, Ar−H *ortho* to I), 7.89 (ddd, 1H, Ar−H *ortho* to S). MS (ESI) *m*/*z*: 535.73 (theory = 535.454 for $[ArINHTs^{tBu}]^+$).

General Procedure for Catalytic Aziridination. To a stirred suspension of ArINTs (580 mg, 1.18 mmol) in benzene (24 mL), a green solution of **1** (10 mg, 0.0098 mmol) in benzene (1 mL) was added to afford a color change to red-brown. Neat styrene (67.5 μL, 0.59 mmol) was added, and the reaction was stirred for 24 h. The reaction mixture was opened to air, and the solvent was removed in vacuo. The residue was separated on a silica column to isolate aziridine.

***N*-(*p*-Tolylsulfonyl)-2-phenylaziridine.** Aziridine was prepared as describe above. Separation was achieved using 1:6 diethyl ether:benzene as eluant. The fractions were collected in 1 mL increments and spotted onto TLC plates. TLC analysis shows aziridine in a spot at R_f = 0.69. Quantitative isolation of aziridine was unsuccessful due to overlapping of the aziridine and ArI (R_f = 0.56) bands from the silica column. The resulting azirdine solid was dissolved in a few drops of diethyl ether and chilled to −20 °C. After 24 h, the supernatant was decanted to give 103 mg of tan crystals (67%). ^{1}H NMR ($CDCl_3$) δ: 2.40 (d, 1H,

(29) HAT from a putative [Fe^{IV}═NR]: (a) Lucas, R. L.; Powell, D. R.; Borovik, A. S. *J. Am. Chem. Soc.* **2005**, *127*, 11596. (b) Eckert, N. A.; Vaddadi, S.; Stoian, S.; Lachicotte, R. J.; Cundari, T. R.; Holland, P. L. *Angew. Chem. Int. Ed.* **2006**, *45*, 6868.
(30) Shriver, D. F.; Drezdzon, M. A. *The Manipulation of Air-Sensitive Compounds*, 2nd ed.; Wiley: New York, 1986; 326 pp.
(31) Heuss, B. D.; Mayer, M. F.; Dennis, S.; Hossain, M. *Inorg. Chim. Acta* **2003**, *342*, 301.
(32) Gross, Z.; Galili, N.; Simkhovich, L.; Saltsman, I; Botoshansky, M.; Bläser, D.; Boese, R.; Goldberg, I. *Org. Lett.* **1999**, *1* (4), 599.

CH_2), 2.42 (s, 3H, CH_3), 2.9 (d, 1H, CH_2), 3.79 (dd, 1H, CH), 7.2−7.36 (m, 7H, Ph, Ts-*m*-H), 7.88 (d, 2H, Ts-*o*-H). mp. 87−88.5 °C (lit. 88−89 °C).[33]

***N*-(*p*-(*tert*-Butylbenzenesulfonyl)-2-phenylaziridine.** Aziridine was prepared as described above. Separation was achieved using 1:3 ethyl acetate:hexanes as eluant. The fractions were collected in 1 mL increments and spotted onto TLC plates. TLC analysis shows aziridine in a spot at $R_f = 0.55$. Quantitative isolation of aziridine was unsuccessful due to overlapping of the aziridine and ArI ($R_f = 0.41$) bands from the silica column. The resulting azirdine solid was recrystallized from hot hexanes to give tan crystals (43%). ^{1}H NMR (C_6D_6) δ: 0.97 (s, 9H, ^{t}Bu), 1.81 (d, 1H, CH_2), 2.73 (d, 1H, CH_2), 3.77 (dd, 1H, CH), 6.96−7.21 (m, 7H, Ph, Ts-*m*-H), 7.96 (d, 2H, Ts-*o*-H) mp. 103−106 °C. MS (CI) *m*/*z*: 316 ([$PhCHCH_2NHTs^{tBu}$]$^+$).

Kinetic Measurements: Kinetics of Formation of 2. Pseudo-first-order kinetic measurements on the formation of **2** were carried out using a stopped-flow analyzer. Equal volumes of solutions of **1** and ArINTs were injected into the chamber and monitored at 600 nm. Reaction profiles were fit to theoretical single-exponential functions to determine the pseudo-first-order rate constants (k_ψ) in accordance with the following relationship: $Abs_t = Abs_\infty + (Abs_0 - Abs_\infty) \exp(-k_\psi t)$. Stock solutions were prepared by dissolving solid **1** and ArINTs in dry benzene (dissolution of poorly soluble ArINTs was encouraged by heating). The limiting solution of **1** (2.54×10^{-5} M) was tested with a range of ArINTs concentrations (3.38×10^{-4}−1.69×10^{-3} M). Because of the limited solubility of ArINTs in benzene, this range could not be expanded to larger concentrations of ArINTs. To widen the range, a further dilution of ArINTs (1.69×10^{-4} M) was examined. For this measurement, **1** was diluted to 1.27×10^{-5} M in order to maintain the 10-fold ArINTs concentration excess necessary for pseudo-first-order kinetics.

Catalytic Aziridination of Olefins: Steady-State Kinetics. To a stirred suspension of ArINTs (58 mg, 120 μmol) in benzene (2 mL), **1** (1.0 mg, 0.98 μmol) in benzene (0.5 mL) was added to afford a color change to red-brown. Neat styrene (6.9 μL, 59 μmol) was added, followed by $(Et_3Si)_2O$ (5 μL) as internal standard. At regular intervals, aliquots of 0.2 mL were removed from the reaction mixture and diluted into 0.5 mL of benzene-d_6 for NMR analysis. Styrene concentrations were determined by comparison between the olefinic ^{1}H peak integrals and those of the internal standard.

Kinetics of Aziridination by Initial Rates Method. Three reactions were prepared for kinetic examination by mixing solutions of ArINTs and **1** with styrene in benzene. Benzophenone (11.4 mM) was used as an internal standard for GC analysis. Initial concentration of ArINTs was varied while all other species were held constant: [ArINTs] = 1.4−12×10^{-4}, [styrene] = 0.025, and [**1**] = 2.0×10^{-5} M. The catalytic reaction was initiated by addition of **1**. After 5 min, 1 μL of solution was drawn and analyzed by GC for the determination of aziridine concentration.

Catalytic Aziridination of Olefins: Competition Kinetics. Aryl-substituted aziridines were prepared in situ according to the general protocol described above. Conversion to aziridine was confirmed by ^{1}H NMR analysis, and retention time for each compound was determined by gas chromatography: *N*-(*p*-tolylsulfonyl)-2-(*p*-trifluoromethylbenzene)aziridine = 14.47 min, *N*-(*p*-tolylsulfonyl)-2-(*p*-chlorobenzene)aziridine = 10.95 min, *N*-(*p*-tolylsulfonyl)-2-(*m*-chlorobenzene)aziridine = 14.93 min. Competition kinetics were carried out by stirring 1 mL of a 0.3 mM solution of **1** (0.3 μmol) with a 1:1 mixture of substituted olefin and styrene (20 μmol of each) and limiting ArINTs (1.0 mg, 2 μmol). These were stirred for 24 h and analyzed by gas chromatography. The integral of each substituted aziridine was compared with that of phenyl aziridine (retention time = 11.61 min). All product ratios were approximately 1.

Double-Labeling Experiment To Determine the Nature of the Oxidizing Species in Aziridination. A vial containing a mixture of **1** (2.1 mg, 2.0 μmol) and $ArINTs^{tBu}$ (1.1 mg, 2.0 μmol) in benzene (1 mL) was stirred until the solution became red-brown (ca. 10 min). This solution was added to a vial containing ArINTs (1.0 mg, 2.0 μmol) and 1.0 mL of a 2.0 mM solution of styrene (2.0 μmol) in benzene. A second reaction was set up in the same way, except that the order of $ArINTs^{tBu}$ and ArINTs was reversed. Both of these were stirred for 8 h and analyzed by GC. *N*-(*p*-(*t*-Butylbenzenesulfonyl)-2-phenylaziridine and *N*-(*p*-tolylsulfonyl)-2-phenylaziridine were identified in the chromatogram by comparison to the known retention times, and the ratio of products was determined by comparison of their respective peak integrals.

Spectroscopy on 2: Absorption spectroscopy on **2** was achieved by stirring a solution of 1 mL of **1** (ca 10^{-3} M) with ArINTs or PhINTs (ca. 1 mg) for 10 min or until the solution was red. The solution was decanted from the solid and analyzed by absorption spectroscopy in a 0.10 mm path length cell. UV−vis (C_6H_6): λ_{max} [nm] (log ϵ) = 360 (sh, 4.48), 404 (4.58), 530 (sh, 3.70).

Mass spectrometry was achieved by evaporation of a toluene solution of **2** (generated from 1 mg of **1** and 2 mg of PhINTs). The microcrystalline solid which formed on the side of the vial was scraped away from the excess PhINTs at the bottom of the vial. The microcrystalline solid was analyzed by ESI mass spectrometry. MS (ESI) *m*/*z*: 861.89 (theory = 862.433 for (tpfc)MnN).

Acknowledgment. The NSF is greatly acknowledged for support of this work (CHE-0443147). We thank Dr. Phillip E. Fanwick for his help with the X-ray structural determinations. We also thank Dr. Jyotishman Dasgupta for his assistance in interpretation of EPR spectra.

Supporting Information Available: Experimental procedures for removal of EtOAc from **1** and corresponding IR spectra; details of magnetic measurements; titration of **1** with EtOAc; ^{19}F NMR and EPR spectroscopy on **2**; ^{1}H NMR and electronic absorption spectroscopy on (tpfc)Mn^V=O; plot of initial rate versus [ArINTs]; synthesis and EPR of (tpfc)Cr^V=NTs; and X-ray structural data for (tpfc)Mn(EtOAc) (**1**) and (tpfc)Cr(NTs). This material is available free of charge via the Internet at http://pubs.acs.org.

JA0665489

(33) Seden, T. P.; Turner, T. W. *J. Chem. Soc. C* **1968**, 876.